Published online 21 March 2013 *Nucleic Acids Research, 2013, Vol. 41, No. 9* ***4813–4824***
doi:10.1093/nar/gkt180

A novel bifunctional histone protein in *Streptomyces*: a candidate for structural coupling between DNA conformation and transcription during development and stress?

Matthew Aldridge, Paul Facey, Lewis Francis, Sion Bayliss, Ricardo Del Sol and Paul Dyson*

Institute of Life Science, College of Medicine, Swansea University, Singleton Park, Swansea SA2 8PP, UK

Received June 18, 2012; Revised and Accepted February 26, 2013

ABSTRACT

Antibiotic-producing *Streptomyces* are complex bacteria that remodel global transcription patterns and their nucleoids during development. Here, we describe a novel developmentally regulated nucleoid-associated protein, DdbA, of the genus that consists of an N-terminal DNA-binding histone H1-like domain and a C-terminal DksA-like domain that can potentially modulate RNA polymerase activity in conjunction with ppGpp. Owing to its N-terminal domain, the protein can efficiently bind and condense DNA *in vitro*. Loss of function of this DNA-binding protein results in changes in both DNA condensation during development and the ability to adjust DNA supercoiling in response to osmotic stress. Initial analysis of the DksA-like activity of DdbA indicates that overexpression of the protein suppresses a conditional deficiency in antibiotic production of *relA* mutants that are unable to synthesise ppGpp, just as DksA overexpression in *Escherichia coli* can suppress ppGpp^0 phenotypes. The null mutant is also sensitive to oxidative stress owing to impaired upregulation of transcription of *sigR*, encoding an alternative sigma factor. Consequently, we propose this bifunctional histone-like protein as a candidate that could structurally couple changes in DNA conformation and transcription during the streptomycete life-cycle and in response to stress.

INTRODUCTION

Dynamic changes to DNA organization in response to physiological and developmental cues are mediated by histones in higher organisms. Here, we describe a novel type of histone-like protein, DdbA, found in complex *Streptomyces* bacteria that undergo a developmental programme and produce a vast range of antibiotics. Gram-positive *Streptomyces* are actinobacteria that typically inhabit terrestrial soils and marine sediments as free-living saprophytes. In a similar manner to a filamentous fungus, these bacteria colonize the particulate environment by growing branching multigenomic hyphae that form a ramifying network enabling the organism to exploit a localized nutrient source. Being non-motile, they achieve dispersal by means of unigenomic spores borne on specialized non-feeding aerial hyphae. The latter grow out of the semi-aqueous environment inhabited by the feeding vegetative hyphae of terrestrial streptomycetes and ultimately undergo multiple coordinated cell division, generating chains of spores. The spores can then be dispersed by physical agents or the activities of motile animals inhabiting the same niche.

A complex regulatory network controls how these bacteria, typified by the model species *Streptomyces coelicolor*, reprogramme their physiology to transit from exponential growth of vegetative hyphae to develop reproductive sporulating aerial hyphae and, usually concomitantly, to produce a diverse array of secondary metabolites (1,2). This regulation is in part dependent on nutritional status and, in response to amino acid or nitrogen limitation, the highly phosphorylated guanosine nucleotide ppGpp accumulates at the end of the exponential phase and during the so-called transition phase that precedes reprogramming (3). Synthesis of this 'alarmone' is directed by *relA* whose transcription correlates with the accumulation of ppGpp. It is evident from global analysis of changes in patterns of transcription, comparing a wild-type and *relA* ppGpp^0 mutant, that this phosphorylated nucleotide is a pleiotropic regulator that redirects transcription from ribosomal RNA synthesis to expression of antibiotic gene clusters and morphogenetic proteins (4), indicative of a genus-specific 'stringent

*To whom correspondence should be addressed. Tel: +44 1792 295667; Fax: +44 1792 295447; Email: p.j.dyson@swansea.ac.uk

response'. The route for how this redirection of gene transcription is mediated has not been determined and hence the importance of investigating functions of DksA-like proteins, the archetype of which is known to augment ppGpp's effect in *E. coli* by impacting on RNA polymerase (RNAP) function (5).

Another feature of *Streptomyces* development is the condensation of chromosomal DNA before segregation of nucleoids into pre-spore compartments. The volume of an unconstrained bacterial chromosome significantly exceeds the volume of the cell where it is contained, hence the need for a packaging mechanism to reduce chromosomal volume sufficiently to make it fit inside the cell. This compaction is achieved by the concerted action of negative DNA supercoiling, molecular crowding and nucleoid-associated proteins (NAPs) (6). In other bacteria, NAPs modulate local DNA conformation as well as the physical structure of the nucleoid. They alter the topology of bound DNA by bending, bridging or wrapping it, leading to multiple effects on the bacterial cell including transcriptional regulation by virtue of making different promoters either more or less accessible to the transcription machinery (7,8). However, we are not aware of evidence for a direct interaction between a bacterial NAP and the core transcription machinery.

Here, we describe an entirely novel bifunctional NAP, DdbA, from *S. coelicolor* that, by virtue of its N-terminal histone-like domain, contributes to organizing DNA conformation during development and in response to stress. The C-terminal half of DdbA consists of a DksA-like domain, and we demonstrate that, just as overexpression of DksA can suppress *E. coli* ppGpp^0 mutant phenotypes (9), overexpression of DdbA restores antibiotic production in *relA* mutants of *S. coelicolor*. DdbA is also required for efficient transcription of the SigR regulon in response to thiol stress, which may parallel the involvement of DksA in *E. coli* in altering RNAP specificity for alternative sigma factors (5). Consequently, we believe that DdbA is a candidate protein that could potentially structurally couple changes in DNA conformation with the transcription machinery.

MATERIALS AND METHODS

Bacterial strains and media

Bacterial strains used in this study are shown in Table 1. Standard culture procedures were used (10,11). Cloning procedures were performed in *E. coli* JM109, whereas *E. coli* ET12567/pUZ8002 was used for intergeneric conjugative transfer of plasmid DNA into *Streptomyces* strains (11). *Streptomyces* mutant strains were obtained using Tn*5062*-mutagenised cosmids (12) (Table 1). The identity of all mutants was confirmed by Southern blot (10). To test diamide sensitivity, 1×10^7 spores of each strain were mixed with soft nutrient agar and evenly poured onto the surface of nutrient agar in standard Petri dishes. A total of 1 mMol diamide was then applied to a sterile filter disc placed on the surface of the agar, before incubation at 30°C for 24 h. Assays were conducted in triplicate.

DNA manipulation and plasmid construction

Cloning procedures were performed using standard protocols (10). Transposant cosmid 4A10.2.D05 was digested with BglII/XbaI, and a 1.8-kb fragment was sub-cloned into pALTER1 to obtain pAL2075. The complementing plasmid pSH2075 was obtained using a SalI/AvrII fragment from pAL2075 encompassing from 636 bp upstream of SCO2075 to 144 bp downstream of the gene's stop codon. This fragment was blunt-ended and ligated to pSH152 previously digested with EcoRV. PCR amplification (Finnzymes Phusion® DNA polymerase) was performed to amplify a fragment spanning from 636 bp upstream of the SCO2075 start codon (forward primer 2075_FWD, XbaI site) to the open reading frame's (ORF) end where the stop codon was replaced by a BglII site (reverse primer 2075_REV). This PCR product was ligated to pGEM-T-Easy to obtain pGEM2075. This plasmid served as the source to excise SCO2075 and its upstream sequence using XbaI and BglII, and this fragment was ligated to pRWHis2 (20) previously digested with XbaI/BamHI to obtain the integrative plasmid p2075His. The latter encodes SCO2075 under its putative native promoter and C-terminally fused to six histidines. The p2075His was used to monitor DdbA expression in *Streptomyces* by immunoblot. The apramycin-resistant marker in p2075His was replaced by a hygromycin resistance gene using the PCR-targeted system (21), resulting in p2075HisH.

The recombinant full-length DdbA expression plasmid (pDksA1) was obtained by PCR amplification of SCO2075 using primers DksA_NdeI (the NdeI site overlaps the start codon) and 2075_REV, digested with NdeI and BglII and ligated to pET26b(+) digested similarly. In parallel, truncated versions of SCO2075 covering the N-terminal and C-terminal domains were amplified by PCR. Primers DksA_NdeI and 2075_trc_BamHI were used to amplify the coding sequence corresponding to the first 138 amino acids and subcloned into pET26b(+) at the NdeI/BamHI sites, resulting in pcDksANTD and expressing DdbA-NTD. Primers CTD_NdeI and 2075_REV were used to amplify the coding sequence corresponding to the 124 amino acids containing the complete C-terminal DksA-like domain, and subcloned into pET26b(+), resulting in plasmid pcDksaCTD and expressing DdbA-CTD. In all the aforementioned plasmids, the resulting translational fusions contain a C-terminal 6xHistidine tag. For overexpression of DdbA::His in *Streptomyces* strains, the PCR amplicon used to generate pDksA1 was digested with NdeI/BglII and subcloned into pRWHis1 previously digested with NdeI/BamHI, generating pDksA3. The apramycin-resistance gene in the latter was replaced with hygromycin resistance using a PCR-targeting system (21) to generate pDksA3H. To overexpress DdbA-NTD, plasmid pcDksANTD was digested with NdeI/BamHI, and the relevant fragment was ligated to similarly digested pRWHis1. The resulting plasmid pDksA4, encoding the DdbA-NTD DNA-binding domain under the control of the *tipA* promoter, was introduced by intergeneric conjugation into *S. coelicolor* M570.

Table 1. Strains, plasmids and cosmids

	Description	Transposon insertion[a] (genome position)	Source/reference
Strain			
S. coelicolor A3(2) M145	Prototrophic SCP1– SCP2– Pgl+		(11)
ddbA	M145 SCO2075::Tn*5062*	SC4A10.1.A08 (2226606)	This study
smc	M145 *Δsmc*::*apra*		(13)
relA	M145 SCO1513::Tn*5062*	9C5.1.C04 (1618604)	This study
M570, *relA*	M600 *relA*::*hyg*		(14)
JM109	F' *traD36 proA*$^+$*B*$^+$ *lacIq Δ(lacZ)M15/ Δ(lac-proAB) glnV44 e14- gyrA96 recA1 relA1endA1 thi hsdR17*		(15)
E. coli ET12567 (pUZ8002)	*dam13*::Tn*9 dcm6 hsdM hsdR recF143* 16 *zjj201* ::Tn*10 galK2 galT22 ara14 lacY1 xyl5 leuB6 thi1 tonA31 rpsL136 hisG4 tsx78 mtli glnV44*, containing the non-transmissible *oriT* mobilizing plasmid, pUZ8002		(16)
Plasmid			
pALTER1	Tetracycline^R		Promega Corp.
pUC18	Ampicillin^R		(15)
pGEM-T-Easy	Ampicillin^R		Promega Corp.
pET-26b(+)	*Kan T7* promoter, C-His-tag expression vector		Novagen
pIJ8600	*tipA* inducible promoter, Apramycin^R		(17)
pIJ8600H	*tipA* inducible promoter, Hygromycin^R		(18)
pROT219	pUWL219, *oriT*		Del Sol, personal communication
pAL2075	pALTER1, SCO2075		This work
pSH152	Hygromycin^R		(19)
pSH2075	Hygromycin^R, SCO2075		This work
pGEM2075	pGEM-T-Easy, SCO2075		This work
pRWHis1	*tipA* promoter, Apramycin^R		(20)
pRWHis2	Apramycin^R		(20)
p2075His	pRWHis2, SCO2075*::His*$_6$ downstream of native promoter		This work
p2075HisH	p2075His, Hygromycin^R		This work
pDksA1	pET-26b(+) containing full length SCO2075 (*ddbA*) coding sequence fused to His tag at C end		This work
pDksA3	SCO2075::[*His*]$_6$ downstream of *ptipA* in pIJ8600		This work
pDksA3H	SCO2075::[*His*]$_6$ downstream of *ptipA*, in pIJ8600H		This work
pDksA4	pRWHis1 containing N-terminal *sco2075* (DdbA-NTD) coding sequence fused to His tag at C end		This work
pcDksANTD	pET-26b(+) containing N-terminal *sco2075* (DdbA-NTD) coding sequence fused to His tag at C end		This work
pcDksaCTD	pET-26b(+) containing C-terminal *sco2075* (DdbA-CTD) coding sequence fused to His tag at C end		This work
p2075mc	pSET152, SCO2075*::mCherry* (*ddbA*::*mCherry*) downstream of native promoter		This work
p2075mcH	p2075mc, Hygromycin^R		This work

[a]http://strepdb.streptomyces.org.uk.

A C-terminal translational fusion to mCherry was constructed by ligating the mCherry coding sequence recovered from pNA585 (22) by digestion with BamHI/EcoRI, an XbaI/BglII SCO2075 fragment form pGEM2075 and pSET152 digested with Xba/EcoRI. The resulting plasmid was named p2075mc. The apramycin-resistant marker in p2075mc was replaced by a hygromycin resistance gene using the PCR-targeted system (21), resulting in p2075mcH. The latter was used to visualize DdbA *in situ* localization.

Monitoring changes in DNA supercoiling

Changes in plasmid topology were analysed as described (23). Briefly, strains containing high-copy number plasmid pROT219 were grown in liquid culture tryptic soy broth (TSB) supplemented with thiostrepton (25 μg/ml) for 24 h and then subjected to osmotic up-shock using 1 M sucrose or 250 mM KCl until enough biomass accumulated (~48 h), when supercoiled plasmid was isolated using an alkaline lysis technique (11). Chloroquine gels were made

using 0.5–1% (w/v) agarose in 1 x Tris-acetate-EDTA buffer (TAE) and containing 6 μg/ml chloroquine. The 1x TAE running buffer also contained 6 μg/ml chloroquine. Supercoiled plasmid DNA was electrophoresed in the dark for 25–40 h at 1–1.5 V/cm, and the buffer was re-circulated to reduce buffer exhaustion at 4°C. Gels were rinsed in 1 mM $MgCl_2$ for 2 h followed by 1 h in dH_2O, then stained for 1 h in 1 μg/ml ethidium bromide followed by a de-staining for 30 min −1 h in dH_2O. Images of chloroquine gels were acquired and analysed using Quantity One software (BioRad). Density traces of each gel lane were constructed and lined up horizontally. Change in linking number (ΔLk) was estimated by counting the number of topoisomers between the most intense distinguishable single topoisomer in the control strain and in the test sample.

Electromobility shift essays

Gel retardation experiments were performed using 300 ng of substrate DNA containing electrophoretic mobility shift analysis (EMSA)-binding buffer (24) [10 mM Tris–HCl (pH 7.5), 80 mM NaCl, 1 mM dithiothreitol (DTT), 1 mM EDTA and 5% glycerol]. The samples were then left at room temperature for 15 min, loaded into a 0.8% agarose 1× TAE gel and run at 4°C at a constant 48 V for 16 h. The gel was stained in 1 μg/ml ethidium bromide, de-stained in dH_2O and visualized using a BioRad gel documentation system.

Microscopy

Fluorescence microscopy was used to visualise DdbA::mCherry and Syto9 stained nucleoids (25). Measurement of length of Syto9 stained nucleoids (~400 nucleoids per strain) was performed using Scion Image software (Scion Corp., Frederick, MD). Data for all nucleoid measurements were initially analysed using the Kolmogorov–Smirnov test for normality. Data that displayed extreme skewness and differed significantly from normality (i.e. $P > 0.05$) were analysed using non-parametric tests. Where significant differences were observed under Kruskall–Wallis tests, pair-wise Mann–Whitney tests were performed post hoc to identify the strain that differed most significantly. All statistic procedures were undertaken in Statistical Package for Social Sciences (SPSS) for windows version 13.0.

Atomic Force Microscopy was used to visualzse DNA condensation by DdbA. Purified DdbA (10, 30 and 50 ng) was incubated with 175 ng of pUC18 DNA, in EMSA-binding buffer. The samples were incubated 30 min at room temperature, diluted 2.5 times with dH_2O and then applied to freshly cleaved mica. After 2 min, the mica was rinsed with dH_2O and dried under a stream of nitrogen. The protein DNA complex was imaged at high resolution using a Nanowizard II (JPK Instruments; Berlin, Germany) Atomic Force Microscope. SNL10 cantilevers were used with a tip diameter of ~10 nm, a spring constant of 0.12 N/m and an optimal resonant frequency between 14 and 26 kHz. All imaging was done in air using no-contact mode.

Protein detection and purification

Total protein samples (10 μg) were separated in 10% SDS–PAGE gels and immunoblotted using an antiHis-HRP conjugate (Qiagen). Protein samples were obtained from cellophane discs placed on top agar plates, followed by sonication in Sonication buffer [50 mM Tris–HCl (pH 7.5), 200 mM NaCl, 15 mM EDTA, complete protease inhibitor cocktail (Roche Diagnostics)] as described (25).

Recombinant expression of full-length and truncated DdbA was achieved in *E. coli* BL21 (DE3). Cells were grown in 2x Yeast extract-tryptone broth (YT) supplemented with 1% glucose and 25 μg/ml kanamycin, shaking at 37°C until OD_{600} reached 0.7, when 1 mM Isopropyl β-D-1-thiogalactopyranoside (IPTG) was added to induce expression, and the culture was transferred to a 30°C shaker incubator for 1 h. Cells were collected by centrifugation, resuspended in binding buffer (50 mM Tris, 500 mM NaCl and 20 mM imidazole at pH 7.5) and sonicated. The protein extract was spun down and filtered through a 0.2 μm filter. The filtered supernatant was then run through a HisTrap column (GE Healthcare) followed by application of 20 ml of wash buffer (50 mM Tris, 500 mM NaCl, 30 mM imidazole, pH 7.5). A stepwise gradient was used to elute the protein in a range of 50, 100, 200 and 300 mM imidazole, with 5 column volumes for each. Samples of each fraction were then assessed by SDS–PAGE and Coomassie staining to verify protein purity and abundance. The protein samples were then dialysed overnight in 50 mM Tris, 80 mM NaCl, pH 7.5. Protein quantification was performed using the Bradford method.

Quantitative Real-Time PCR

Total RNA extraction, cDNA synthesis and quantitative real-time PCR (qRT-PCR) were performed as described (26). Oligonucleotides were designed using Beacon Design (Premier Biosoft, USA) and shown in Table 2. PCR reaction specificity was assessed using melt curve analysis. Transcript abundance was estimated using a standard curve generated with serial dilutions of *S. coelicolor* genomic DNA. *S. coelicolor hrdB* was used as internal control to normalize samples. Normalized starting quantities were initially tested for normality using the Kolmogorov–Smirnov test. Significant differences between transcript abundance among strains were tested using a one-way ANalysis Of VAriance (ANOVA). All statistical analysis procedures were performed in SPSS version 16 for Windows.

Bioinformatic analyses

Amino acids sequences used for analysis were retrieved from NCBI (http://www.ncbi.nlm.nih.gov), Microbial Genome Database (MBGD) (http://mbgd.genome.ad.jp), Broad Institute (http://www.broadinstitute.org) and organism-specific genome sequence databases. Sequence alignments were generated using ClustalW2. Secondary structure predictions were performed using JPred (http://www.compbio.dundee.ac.uk/www-jpred/).

Table 2. Oligonucleotides

Name	Sequence 5′–3′
2075_FWD	AATCTAGACGCGCCAGAAGTCGAGCA
2075_REV	AAAGATCTGCGTACCGGCGCTCCTGC
DksA_NdeI	AACATATGGTGGCGAAGAAGAAGACG
2075_trc_BamHI	AAAGGATCCTCGATCTCGGTGCGCA
CTD_NdeI	AAACATATGGGCGAGGAACCCTGGACC
SigR_RTF1	GCGTCCTTCCACCAGTTCC
SigR_RTR1	CTTCTTGCGGTACGAGTTGATG
hrdBFor	CCTCCGCCTGGTGGTCTC
hrdBRev	CTTGTAGCCCTTGGTGTAGTC
SCO3874GyrBF	CGCTATCACAAGATCATCC
SCO3874GyrBR	GAACAGGAAGGTCAGCAG

RESULTS

The product of SCO2075 is a novel DksA-like protein with an N-terminal DNA-binding histone H1-like domain

A Blastp search of *S. coelicolor* proteins revealed three paralogues of the *E. coli* DksA protein: SCO2075, SCO6164 and SCO6165, with *e*-values of 8×10^{-11}, 2×10^{-08} and 1×10^{-06}, respectively. The most conserved of the three has an elongated N-terminal sequence extending an additional 93 amino acids, which interestingly contains a predicted histone H1-like DNA-binding domain (Supplementary Figure S1). The other two DksA paralogues, SCO6164 and SCO6165, are encoded by genes that form a likely operon, and encode proteins of similar size as *E. coli* DksA. Using ClustalW2, the three protein sequences were aligned with that of *E. coli* DksA. A characteristic four cysteine-zinc finger domain of *E. coli* DksA is conserved in all three paralogues. SCO2075 also has two highly conserved polar aspartic acid residues equivalent to those in *E. coli* DksA at positions 71 and 74. In SCO6164, these residues are both substituted by the neutral non polar amino acid leucine, and in SCO6165, one aspartic acid residue is conserved, and the other has been replaced by isoleucine (Supplementary Figure S2). Jpred predictions of secondary structures revealed similar architectures of a long alpha helix and two small C-terminal helices in the aligned regions of the proteins (Supplementary Figure S2).

The SCO2075 gene is located within the conserved core region of the *S. coelicolor* linear chromosome in close proximity to the cell division gene *ftsZ* (SCO2082). This location is common to 19 fully sequenced streptomycete genomes, with no exceptions, although there is variability in the length of the N-terminal predicted DNA-binding domain among the various streptomycete orthologues. In contrast, the other DksA-like paralogues are less well conserved, with 11 species encoding SCO6164 orthologues and 9 species with SCO6165-like proteins. SCO2075 orthologues were only found in streptomycete genomes. The 93-residue N-terminal domain of SCO2075 is a highly basic sequence of amino acids with a pI of 10.5. A Blastp search with this sequence revealed similarity with histone H1Hc2-like protein from *Chlamydia trachomatis* (*e*-value 1×10^{-14}) and the HU-like protein with an extended C-terminal domain, HupS, of *S. coelicolor* (*e*-value 5×10^{-14}), the extended C-terminal domain of which itself shares similarity to H1 histones. The similarity of SC02075 with H1 histones is with the C-terminal linker DNA-binding region of the latter and includes five lysine-rich pentapeptide repeats of S/T, A/T, A, K, K that resemble the conserved S/T, P, K, K tetrapeptide repeats of this region of H1 histones (27).

To analyse the DNA-binding ability of SCO2075, three different His-tagged recombinant proteins were produced: full-length SCO2075, a 138 amino acid protein consisting of the predicted N-terminal DNA-binding domain and a 124 amino acid protein containing the complete C-terminal DksA-like domain (Supplementary Figure S1). EMSAs using supercoiled plasmid DNA revealed gel retardation by both the full-length and the N-terminal domain proteins, but not by the C-terminal DksA-like domain (Figure 1). Similar results were obtained with linearized plasmid DNA (results not shown). Hereafter, the product of *SCO2075* is referred to as DdbA (Dks-like DNA-binding protein).

DdbA contributes to nucleoid condensation during sporulation

To examine *ddbA* function *in vivo*, a null mutant was constructed with a Tn*5062* insertion 77 bp after the start of the gene. With respect to its macroscopic phenotype, the mutant did not differ from the wild-type in terms of sporulation. In addition, a mCherry translational fusion was constructed to determine time of expression and localization of the protein by fluorescence microscopy. The gene encoding the fusion protein restored normal growth of the *ddbA* mutant grown under osmotic stress (see later in the text), indicating functionality. Under control of the native promoter, the mCherry-tagged protein is abundant in spores before and immediately after germination, with the protein apparently diffusing along the young hyphae (Figure 2). However, beyond a short distance from the germinated spore and in older vegetative hyphae, there was very little detectable fluorescent signal, indicating low levels of expression and/or rapid turnover of the fusion protein. Only during growth and development of aerial hyphae was the mCherry fusion protein detectable once again, with the intensity of the signal increasing as the aerial hyphae matured (Figure 2). The protein appears to be nucleoid-associated within pre-spores as the diffuse nature of the protein evident in early aerial hyphae changes to co-localization with condensing nucleoids during early sporulation. During late sporulation, when the unigenomic spores are mature, the localization of the DdbA::mCherry fusion protein is consistent with the shape of the nucleoid (Figure 2). This association was confirmed by examining localization of the fusion protein in a *smc* null mutant that generates nucleoid-free spore compartments at high frequency (13). Little or no fusion protein could be detected in anucleate cells (Figure 2). In addition to the cytological analysis, the developmental regulation of DdbA was confirmed by western blot, indicating abundant expression of the His-tagged protein (that

retained function from evidence of complementation of the osmotic stress-induced phenotype of the *ddbA* mutant—see later in the text) under the control of the native promoter after 72 h growth and in spores (Figure 2). The 25 kDa DdbA protein from both *S. coelicolor* and purified from *E. coli* migrates slower than predicted in SDS–PAGE gels.

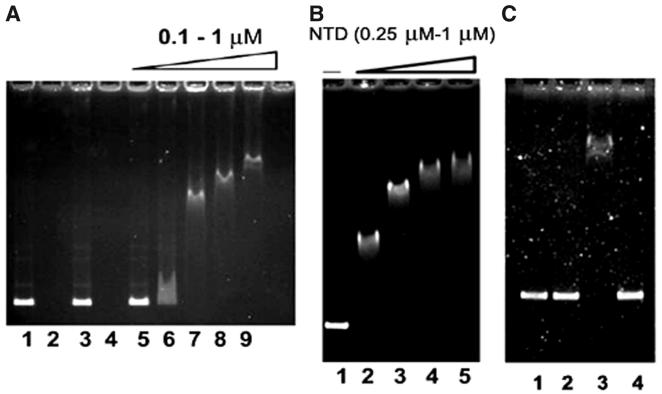

Figure 1. DdbA is a DNA-binding protein as revealed by EMSA. Panel A: Lane 1 contain 300 ng pUC18 supercoiled DNA substrate in the absence of protein, lane 2: 1 μg BSA, lane 3: 1 μg BSA and 300 ng DNA, lane 4: 1 μg DdbA. Lanes 5 and 6 contain pUC18 substrate DNA with DdbA in a range of 0.1, 0.25, 0.5, 0.75 and 1 μM of protein. The open triangle on the top of the gel image indicates DdbA protein concentration range used. Panel B: Reactions were performed with 300 ng of pUC18 as substrate DNA in the absence of protein (lane 1) or in the presence of 0.25, 0.5 0.75 or 1 μM of DdbA-NTD protein (lanes 2–5). The open triangle on the top of the gel image denotes increasing concentrations of the protein. Panel C: All lanes contain 300 ng supercoiled plasmid pUC18 substrate DNA and respectively no protein (lane1), 1 μM DdbA-CTD protein (lane 2), 1 μM full-length DdbA protein (lane 3) and 1.8 μM DdbA-CTD protein (lane 4).

The association of DdbA with compacting chromosomes during sporulation led us to compare the nucleoids of the null mutant and wild-type. The dimensions of 400 pre-spore nucleoids stained with Syto9 were determined for each strain, including the genetically complemented mutant (Figure 3). Average nucleoid lengths were 0.78 μm, 0.89 μm and 0.8 μm for the wild-type, the null mutant and the complemented mutant (not shown), respectively, with the length differences between nucleoids of the mutant and the other strains being statistically significant (using Kruskall–Wallis tests and pair-wise Mann–Whitney tests). Aside from the apparent length difference, the less condensed nucleoids of the mutant often appeared 'boxier' or 'bilobed' compared with those of the other strains (Figure 3). No differences were seen for either the dimensions of pre-spore compartments or the frequency of anulceate cells between these strains.

Recombinant DdbA was also observed to condense supercoiled plasmid DNA *in vitro*. Atomic force microscopy of protein–DNA assemblies revealed different sized complexes of multiple plasmid molecules condensed with oligomeric protein (Figure 4), resembling electron micrograph images of other histone H1-like proteins condensed with plasmid DNA (28).

DdbA alters DNA topology in response to osmotic stress

The only discernable macroscopic phenotype of the *ddbA* null mutant was both a delay in sporulation and concomitant increase in production of the antibiotic actinorhodin compared with either the wild-type or complemented

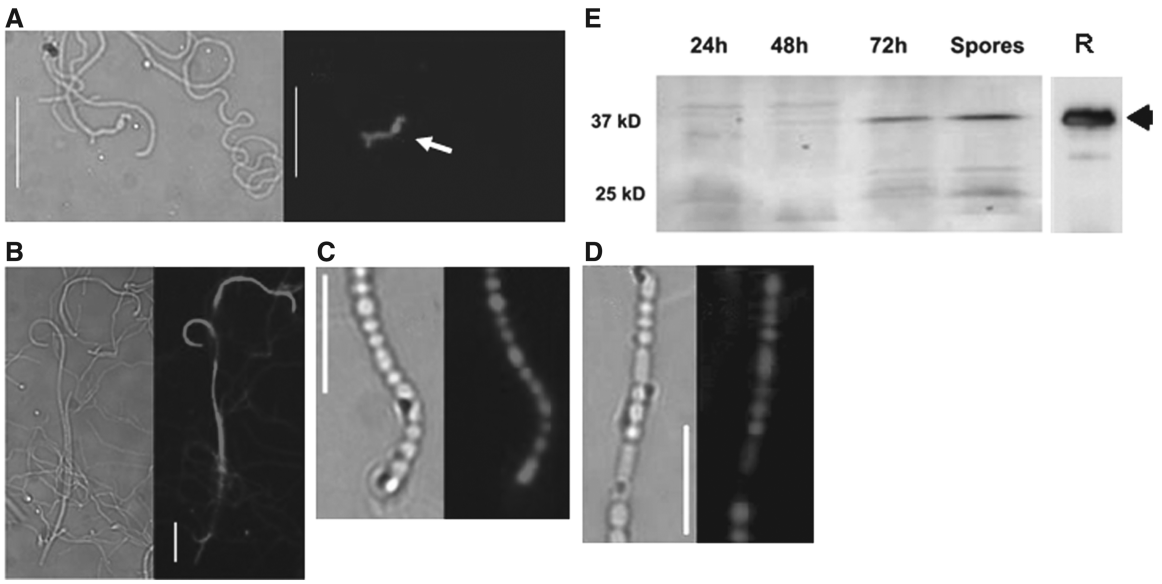

Figure 2. DdbA is a developmentally regulated NAP. Panel A: DdbA::mCherry is present in a germinating spore (arrowed) and in a small region of the adjacent young aerial hyphae. Panel B: DdbA::mCherry is subsequently expressed in non-branching aerial hyphae. Panel C: DdbA::mCherry co-localizes with nucleoids in spore compartments. Panel D: little or no fusion protein was detected in nucleoid-free spore compartments of an *smc* mutant. Bars indicate 10 μm. Panel E: total protein extracts from *S.coelicolor* M145/ p2075His grown on the surface of SFM plates were collected and immunobloted. Spores were collected after 4 days, filtered through cotton and a total protein extract prepared. In all, 10 mg of total protein were loaded in each of the first four lanes. Adjacent panel (R) shows purified recombinant DbdAHis expressed in *E.coli* BL21 (DE3), and detected as above.

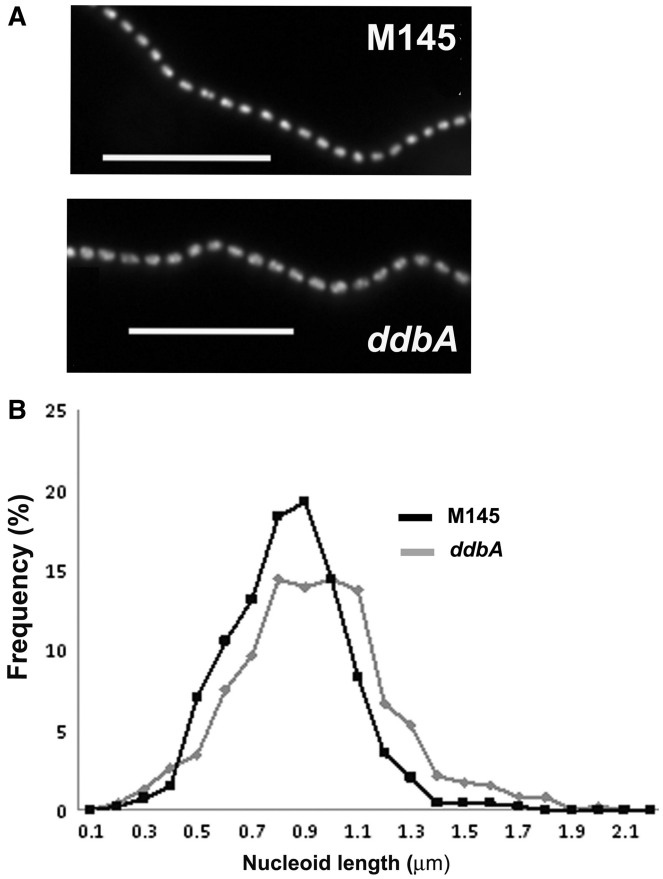

Figure 3. DdbA contributes to nucleoid condensation during sporulation. Panel A: representative images of live-stained nucleoids from *S.coelicolor* M145 and the *ddbA* mutant. Bars indicate 10 μm. Panel B: histogram showing distribution of nucleoid sizes in these strains (a minimum of 400 nucleoids measured per strain). The histogram was generated by plotting the percentage of nucleoids per 0.1 mm size intervals, across the 0.1–3 mm size interval.

mutant when these strains were grown on media containing 250 mM potassium chloride (Figure 5). To explore this link further, expression of *ddbA* was quantified by qRT-PCR, indicating that it is induced during vegetative growth slightly >2-fold (significantly different, one-way ANOVA, $P < 0.05$) 60 min after osmotic stress (Figure 5). This induction implies another aspect of the gene's regulation, in addition to its developmental control.

Certain nucleoid-associated proteins in other bacteria have the ability to affect DNA topology and thereby influence gene expression in response to changes in osmotic conditions (8). Moreover, using a reporter plasmid to monitor DNA supercoiling, an increase in negative supercoiling was observed in *S. lividans* grown in the presence of increased osmolyte (23). We investigated the influence of DdbA on changes to DNA supercoiling in response to varying osmolyte concentration using a similar approach. As observed in *S. lividans*, 2 day growth of the M145 *S. coelicolor* wild-type strain in the presence of 1M sucrose results in a net increase in the mean linking number (~ΔLk) of plasmid supercoils of +6 (Figure 6). In the *ddbA* null mutant, however, no detectable osmolyte-induced increase in negative supercoiling was observed; the difference in mean linking number between the mutant and M145 under osmotic stress was ~ΔLk −4, −7 and −6 for 0.72 M sucrose, 1 M sucrose and 250 mM KCl, respectively. To confirm the apparent role of DdbA in altering DNA supercoiling, plasmid DNA from the complemented mutant grown in medium supplemented with osmolyte was analysed. In this strain, we observed a similar increase in negative supercoiling as seen for the wild-type (Figure 6).

We investigated whether these differences in osmolyte-induced DNA topology are related to transcription of *gyrB*, encoding a subunit of DNA gyrase that introduces negative supercoiling. In the wild-type, we observed rapid induction, with a 2.8- to 3.5-fold increase in transcript abundance between 5 and 15 min after osmotic shock (Figure 6). In contrast, little or no induction was detected in the *ddbA* mutant. Before induction and 60 min after osmotic stress, there was no significant difference in expression between the wild-type and mutant, indicating that regulation of *gyrB* is only one aspect for how DdbA impacts on DNA supercoiling.

DdbA can function both upstream and downstream of *relA*, responsible for ppGpp synthesis

In *E. coli*, DksA augments the role of ppGpp in the stringent response and consequently has been termed a ppGpp cofactor (29). In addition, overexpression of DksA can suppress the phenotypes of $ppGpp^0$ mutants (9). In *S. coelicolor*, ppGpp is synthesised towards the end of exponential growth and during the so-called transition phase immediately before antibiotic production; a *relA* mutant is conditionally deficient in antibiotic production (14). We investigated overexpression of *ddbA* in *S. coelicolor relA* mutants constructed in two different genetic backgrounds. DdbA was overexpressed by fusing the gene to the thiostrepton-inducible *tipA* promoter in pIJ8600 or pIJ8600H, and consequently all strains tested contained either the empty vector or the *ddbA* overexpression plasmid. As our previous experiments were performed in M145, we constructed a mutant containing a Tn*5062* insertion in *relA* and tested two independent isolates of this mutant. Although M145 produced red prodigines on nitrogen-limiting supplemented minimal medium, solid (SMMS) medium, the independently isolated *relA* mutants did not (Figure 7a). The second genetic background we tested was *S. coelicolor* M570, using a previously published *relA* mutant (30). The parental M570 produced actinorhodin on SMMS, whereas the mutant did not (Figure 7b). In both mutants containing a *ddbA* overexpression plasmid, antibiotic production was restored in response to addition of inducer to the growth medium; overexpression of *ddbA* triggered production of red prodiginines in the M145 genetic background and blue actinorhodin in the M570 background (Figure 7). To test whether this apparent suppression of the phenotype of the M570 *relA* mutant could be attributed to the DksA-like domain of DdbA, we also overexpressed just the 138 amino acid N-terminal DNA-binding domain of the protein. Antibiotic production was not restored in the mutant, indicating that the full-length protein is required

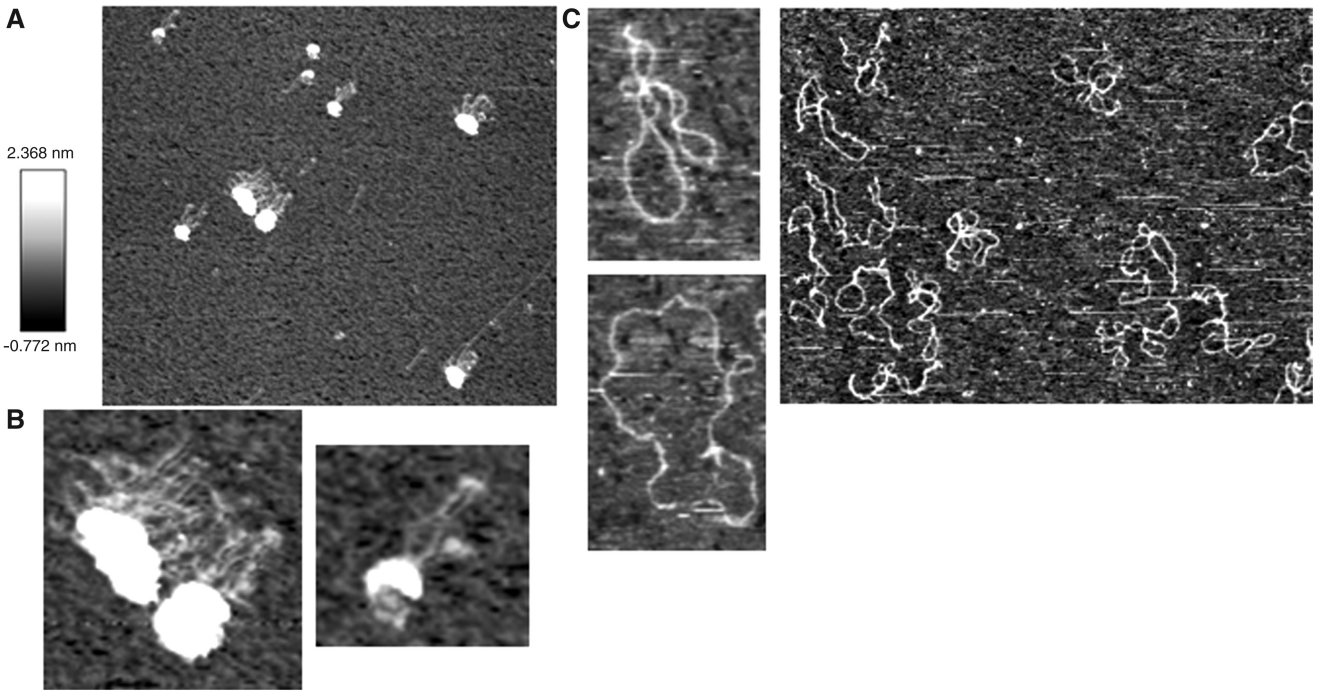

Figure 4. *In vitro* condensation of plasmid DNA by DdbA. Panel A: Atomic Force Microscopy image (Height) of DdbA bound to circular pUC18 plasmid. Panel B shows enlargements of a large-, an intermediate- and a smaller-sized protein–DNA aggregate. Panel C illustrates circular pUC18 (negative control).

for *relA* suppression (results not shown). Overexpression of either full-length DdbA or the N-terminal DNA-binding domain in M145 did not affect antibiotic production.

In *E. coli*, ppGpp/DksA-dependent remodelling of transcription is in part mediated by alternative sigma factors changing the promoter specificity of RNAP (5). For alternative sigma factors such as Sig^S and Sig^N, a sigma competition model has been proposed whereby ppGpp/DksA alters the specificity of interaction of the housekeeping Sig^{70} to core RNAP, allowing other sigma factors to bind (31). We discovered that the *ddbA* mutant is sensitive to diamide, a thiol-specific oxidising agent, and this sensitivity is restored by genetic complementation with *ddbA* (Table 3). In streptomycetes, thiol oxidation is sensed by a complex of the alternative sigma factor, SigR, bound to its antisigma factor RsrA (32). Disulphide bond formation in RsrA causes conformational changes, releasing SigR that directs RNAP to transcribe genes belonging to the SigR regulon that include *sigR* itself, the *trxAB* operon encoding thioredoxin reductase and thioredoxin, and the *relA* gene (33), the latter encoding an enzyme that is the principal ppGpp synthase. To investigate the sensitivity of the *ddbA* mutant to thiol stress and its relation to *sigR* expression, the induction of the gene after exposure to diamide was quantified in the wild-type and mutant, indicating impaired upregulation of *sigR* in the mutant (Figure 8). No significant differences in very low, uninduced, levels of expression between wild-type and mutant were detected. Hence, the sensitivity of the mutant to thiol stress is likely due to reduced expression of the SigR regulon.

DISCUSSION

The most conserved DksA-like protein in *Streptomyces*, DdbA, is composed of two halves. The C-terminal half aligns with other DksA proteins, sharing the characteristic four cysteine-zinc finger domain and two aspartic acid residues that are proposed to stabilize ppGpp binding to RNAP by mutual coordination of an Mg^{2+} ion that is crucial for RNA polymerization (34). The N-terminal half, however, is specific to streptomycete DdbA orthologues and comprises a histone H1-like DNA-binding domain. *S. coelicolor* encodes two other DksA-like proteins, the products of SCO6164 and SCO6165. The subtle macroscopic phenotype of a *ddbA* mutant may be because of functional redundancy shared with these genes.

Developmental regulation of DdbA coincides with the onset of aerial hyphal development leading to sporulation, and the protein is involved in subsequent nucleoid condensation. Several NAPs have been identified that contribute to the programmed chromosomal condensation that is a necessary process to ensure segregation of nucleoids during cell division (2). The N-terminal histone H1-like DNA-binding domain of DdbA confers the ability for efficient DNA binding to both circular supercoiled and linear plasmid DNA *in vitro*. A feature of this domain is the five lysine-rich pentapeptide repeats of S/T, A/T, A, K, K that resemble the three conserved S/T, P, K, K tetrapeptide repeats of the linker-binding region of eukaryotic H1 histones. The 34 amino acid segment encompassing the three repeat units is responsible for DNA condensing properties of H1 and as such has been

termed the DNA-condensing segment (27). Atomic force microscopy of DdbA bound to supercoiled plasmid DNA revealed different sized aggregates of the protein and DNA. Larger complexes are indicative of participation of several plasmid molecules bound at a condensed centre of oligomeric DdbA, surrounded by unbound DNA loops. Although this indicates that DdbA can form high molecular weight complexes with DNA, just

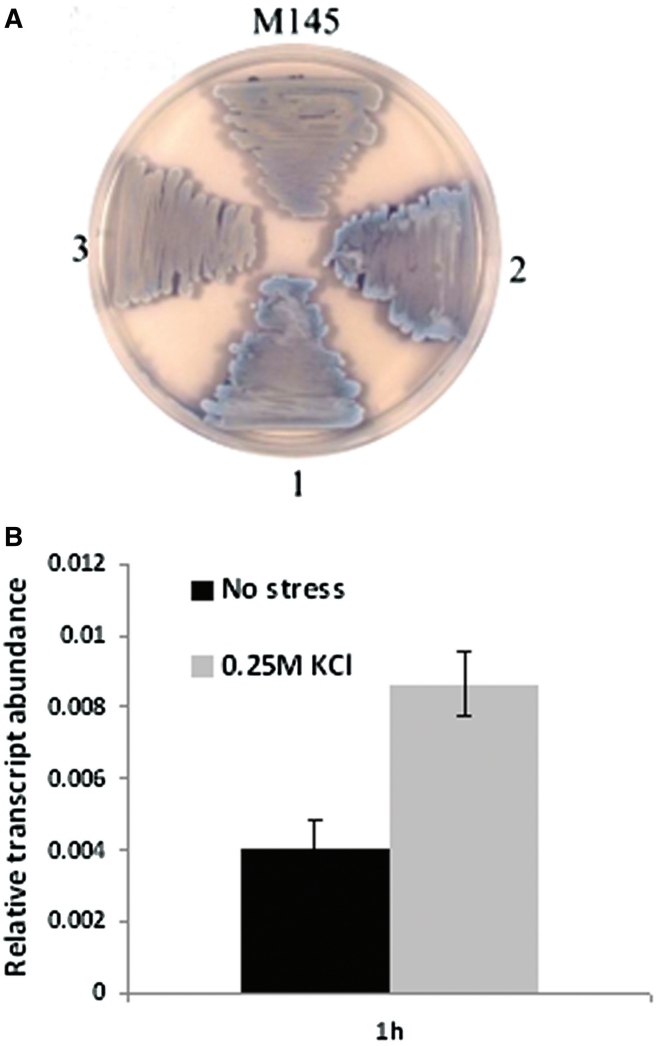

Figure 5. The *ddbA* is involved in the osmotic stress response. Panel A: increased production of blue actinorhodin as a result of osmotic stress was evident with surface grown cultures of the *ddbA* mutant (1) and the mutant with an empty vector, pSH152 (2), compared with the genetically complemented mutant containing plasmid pSH2075 (3). The wild-type strain, M145 is also shown for comparison. M145 containing pSH152, not shown, has a similar phenotype to the plasmid-free wild-type strain. The strains were grown on NMMP medium containing 250 mM KCl. Panel B: qRT-PCR quantifying *ddbA* transcript abundance before and after of osmotic up-shock with 250 mM KCl. *S.coelicolor M145* was grown for 16 h on cellophane discs on the surface of MS agar and then transferred to MS/250 mM KCl plates and incubated for 1 h before total RNA extraction. A non-stressed control sample was processed in parallel by transfer of a cellophane disc to an MS plate, followed by 1 h incubation. The data represent averages obtained from three biological replicates, with three experimental replicates performed on each sample.

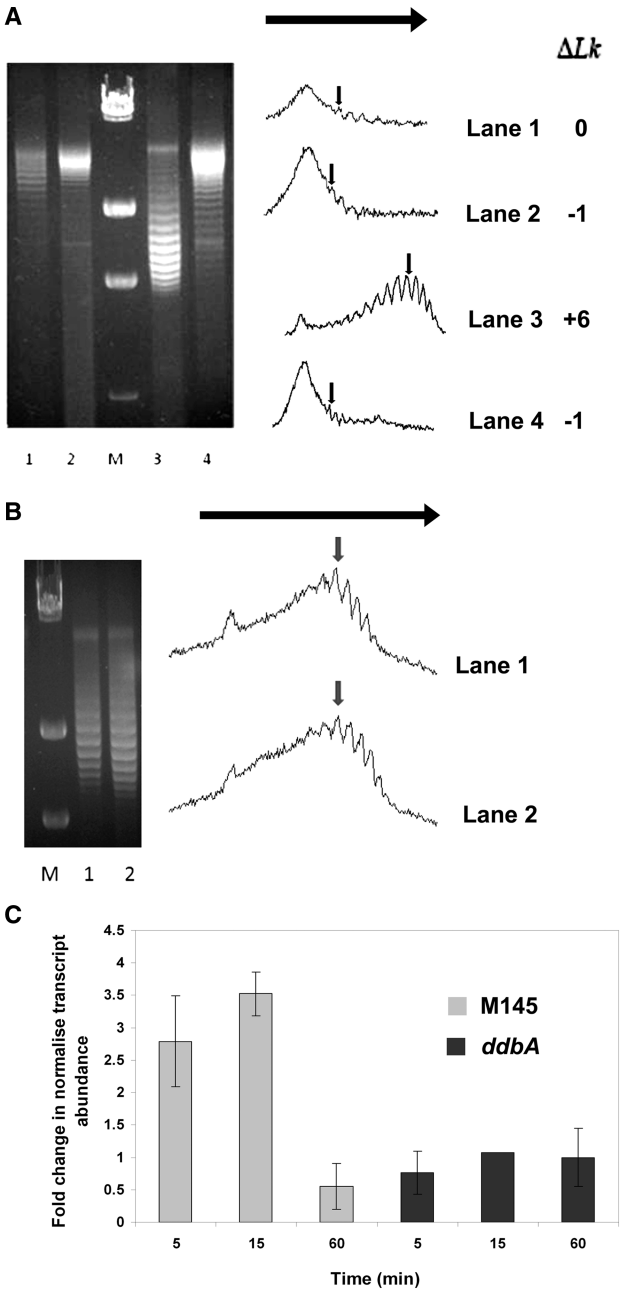

Figure 6. DdbA modulates DNA supercoiling. For panels A and B, plasmid pROT219 DNA was extracted and supercoils separated on chloroquine gels together with HindIII restricted λ DNA (lane M). Quantitation of the intensity of bands corresponding to individual topoisomers from each lane is shown next to each gel. Lkm, the most abundant topoisomer is indicated by the vertical arrow and the change in linking number, ΔLk is shown for each lane using plasmid isolated from M145 with no osmolyte (Panel A, lane 1) as a reference point. The horizontal arrow indicates direction of migration in gel. Panel A: Lanes 1 and 3—plasmid from M145 grown without and with 1 M sucrose; lanes 2 and 4—plasmid from the *ddbA* mutant grown without and with 1 M sucrose. Panel B: lane 1—plasmid from the M145 parental strain grown with 1 M sucrose; lane 2—plasmid from the genetically complemented *ddbA* mutant with integrated pSH2075 grown with 1 M sucrose. Panel C: qRT-PCR quantifying *gyrB* transcript abundance in strains M145 and the *ddbA* mutant before and after of osmotic up-shock with 250 mM KCl. *S.coelicolor* M145 was grown for 16 h on cellophane discs on the surface of MS agar and then transferred to MS/250 mM KCl plates and incubated for between 5 and 60 min before total RNA extraction. The data represent averages obtained from three biological replicates, with three experimental replicate performed on each sample.

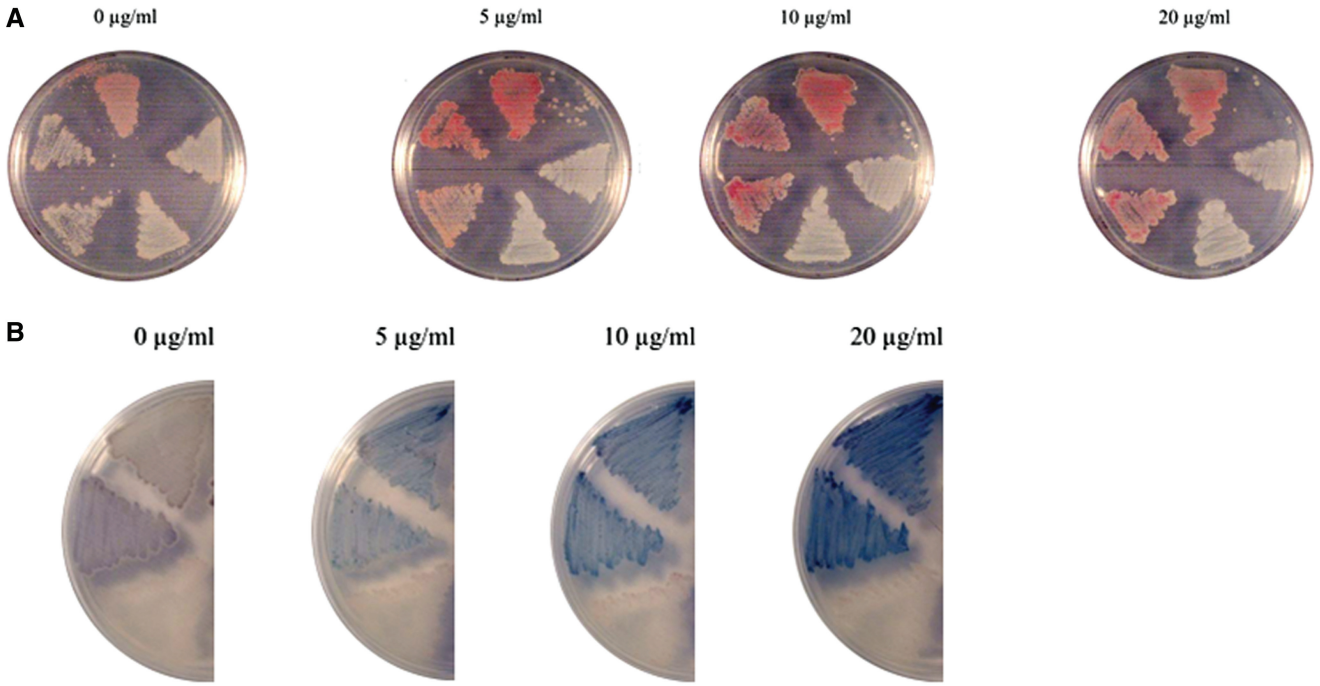

Figure 7. Over-expression of DdbA restores antibiotic production in *relA* mutants. Strains were grown for 5 days on SMMS medium supplemented with indicated concentrations of the inducer, thiostrepton. Panel A: clockwise from top: M145 with the empty vector pIJ8600H; two independent *relA* mutants of M145 with the empty vector pIJ8600H; the same two *relA* mutants with plasmid pDksA3H. Panel B: the top two strains are two independent clones of M570*relA* with plasmid pDksA3; the bottom strain is M570*relA* with the empty vector pIJ8600.

Table 3. Sensitivity to diamide (1 mMol)

Strain	Diameter of inhibition zone (mm)
ddbA	28.33* ± 1.53
ddbA + pSH152	28.67* ± 1.52
M145	22.17 ± 0.76
M145 + pSH152	22.91 ± 0.46
ddbA + pSH2075	23.67 ± 0.58

*Significant ($P < 0.05$) difference as determined using Kruskal–Wallis test.

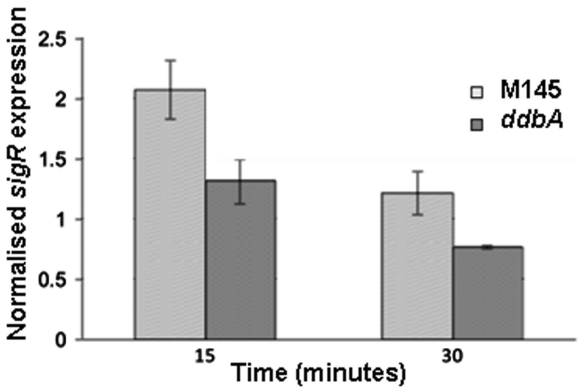

Figure 8. Reduced induction of *sigR* expression in a ddbA mutant. The qRT-PCR analysis of *sigR* transcript abundance at 15 and 30 min after induction of thiol stress in M145 and the *ddbA* mutant. The data were normalized using *hrdB* as a control. Strains were grown over night on NMMP and transferred to minimal liquid medium (NMMP) + 0.5 mM diamide. The data represent averages obtained from three biological replicates, with three experimental replicate performed on each sample.

how it contributes to nucleoid condensation *in vivo*, in conjunction with other streptomycete NAPs, remains to be determined.

In *E. coli* topological alterations of DNA are normally associated with growth transitions (35) and genome-wide transcriptional remodelling (36), but the regulatory mechanisms that coordinate the response of global transcription to variations in DNA supercoiling remain largely undetermined. DNA supercoiling is under the control of a homeostatic network comprising DNA topoisomerases, abundant NAPs and the components of the transcription machinery (8). Mutations of NAPs can alter both the overall superhelicity and the transcriptional response to variations in supercoiling (36). Our investigations into DdbA function in *S. coelicolor* indicate that this NAP plays an important role in regulating DNA topology as evidenced from examining supercoiling after osmotic stress. The *ddbA* mutant, in contrast to the wild-type, is unable to increase negative supercoiling in conditions of high osmolyte concentration when *ddbA* expression is normally upregulated. At least two factors contribute to the difference in DNA topology. First, immediate upregulation of gyrase after osmotic stress is compromised in the mutant. Second, as indicated from DNA supercoiling assays on plasmid DNA isolated from cultures grown with osmolyte for 2 days, DdbA is required for maintaining the increased level of negative supercoiling. We have

not observed any *in vitro* topoisomerase activity of DdbA itself. The experimental conditions for *in vivo* supercoiling analysis were chosen to provide evidence of very obvious changes to DNA topology; it is unclear as yet how *Streptomyces* remodel their DNA topology during growth transitions, although it is likely that both developmental nucleoid condensation and a switch to secondary metabolism, affecting intracellular ATP/ADP ratios, involve topology changes.

In *E. coli*, a ppGpp^0 mutant has multiple amino acid requirements and is affected in cell aggregation and motility (37). These phenotypes can be suppressed by overexpression of DksA, indicating that the protein, in sufficient quantity, can function independently of ppGpp in regulating gene expression by direct interaction with RNAP (9). A phenotype of *S. coelicolor relA* mutants is an inability to synthesise antibiotics when grown in conditions of nitrogen limitation (14). We observed dose-dependent suppression of this conditional antibiotic production deficiency of *relA* mutants owing to overexpression of full-length DdbA, but not when the N-terminal DNA-binding domain alone was overexpressed. We are currently investigating whether these phenotypic data are indicative of a direct interaction of DdbA with RNAP, independent of ppGpp, modifying its activity so that antibiotic biosynthetic gene clusters are transcribed.

The *S. coelicolor relA* gene has two promoters, one of which (p1) is constitutive, whereas the second (p2) is induced in transition phase when levels of intracellular ppGpp increase (30). The *relAp2* is a target for the extracytoplasmic function (ECF) sigma factor SigR after disulphide stress (33). The *relA* transcription was also recently found to be induced in conditions of nitrogen limitation by another ECF sigma factor SigT, although whether *relAp2* is the target promoter in this case, as is likely, was not determined (38). In *E. coli*, ppGpp/DksA-dependent remodelling of transcription is in part mediated by alternative sigma factors changing the promoter specificity of RNAP (5). For alternative sigma factors such as Sig^S and Sig^N, a sigma competition model has been proposed whereby ppGpp/DksA alters the specificity of interaction of the housekeeping Sig^{70} to core RNAP, allowing other sigma factors to bind (31). In addition, the inhibition of transcription of rRNA promoters is believed to increase core RNAP availability for binding with alternative sigma factors. Besides this indirect ppGpp/DksA-dependent mechanism, there is also evidence for a direct role of ppGpp and DksA in activating transcription by the ECF sigma factor SigE bound to RNAP *in vitro* (39). In light of these dependencies between alternative sigma factor function and ppGpp/DksA in *E. coli*, we explored the relationship between the sensitivity of the *ddbA S.coelicolor* mutant to disulphide stress and *sigR* expression, itself dependent on SigR (33). The reduction in *sigR* expression in the mutant after disulphide stress suggests a partial dependence, either direct or indirect, on ppGpp/DdbA for activation of the SigR regulon. This dependence helps to explain why *relA* is part of this regulon as an increase in ppGpp synthesis would help sustain the SigR-dependent disulphide stress response.

In conclusion, the combined results indicate that the histone-like DdbA is a candidate for a NAP that could structurally couple changes in DNA conformation with the transcription machinery. The focus of these investigations has been primarily on the DNA-binding function of this protein during development and in response to stress. We are now continuing to investigate the function of the DksA-like domain and how it can modulate RNAP activity. As far as we are aware, this is the first example of a NAP that can potentially couple these two fundamental processes.

SUPPLEMENTARY DATA

Supplementary Data are available at NAR Online: Supplementary Figures 1–2.

ACKNOWLEDGEMENTS

The authors thank Dagmara Jakimowicz, Jolanta Zakrzewska-Czerwinska and Mervyn Bibb for kindly supplying *Streptomyces* mutants.

FUNDING

European Commission [FP6, LSH-IP 005224, ActinoGen]; European Social Fund grant (to M.A.). Funding for open access charge: Swansea University.

Conflict of interest statement. None declared.

REFERENCES

1. Martin,J.F. and Liras,P. Engineering of regulatory cascades and networks controlling antibiotic biosynthesis in *Streptomyces*. *Curr. Opin. Microbiol.*, **13**, 263–273.
2. McCormick,J.R. and Flardh,K. Signals and regulators that govern *Streptomyces* development. *FEMS Microbiol. Rev.*, **36**, 206–231.
3. Hesketh,A., Sun,J. and Bibb,M. (2001) Induction of ppGpp synthesis in *Streptomyces coelicolor* A3(2) grown under conditions of nutritional sufficiency elicits actII-ORF4 transcription and actinorhodin biosynthesis. *Mol. Microbiol.*, **39**, 136–144.
4. Hesketh,A., Chen,W.J., Ryding,J., Chang,S. and Bibb,M. (2007) The global role of ppGpp synthesis in morphological differentiation and antibiotic production in *Streptomyces coelicolor* A3(2). *Genome Biol.*, **8**, R161.
5. Potrykus,K. and Cashel,M. (2008) (p)ppGpp: still magical? *Annu. Rev. Microbiol.*, **62**, 35–51.
6. Luijsterburg,M.S., Noom,M.C., Wuite,G.J. and Dame,R.T. (2006) The architectural role of nucleoid-associated proteins in the organization of bacterial chromatin: a molecular perspective. *J. Struct. Biol.*, **156**, 262–272.
7. McLeod,S.M. and Johnson,R.C. (2001) Control of transcription by nucleoid proteins. *Curr. Opin. Microbiol.*, **4**, 152–159.
8. Dillon,S.C. and Dorman,C.J. Bacterial nucleoid-associated proteins, nucleoid structure and gene expression. *Nat. Rev. Microbiol.*, **8**, 185–195.
9. Magnusson,L.U., Gummesson,B., Joksimovic,P., Farewell,A. and Nystrom,T. (2007) Identical, independent, and opposing roles of ppGpp and DksA in *Escherichia coli*. *J. Bacteriol.*, **189**, 5193–5202.
10. Sambrook,J.D.W.R. (2001) *Molecular cloning: a laboratory manual*. Cold Spring Harbor Laboratory Press, New York.

11. Kieser,T., Bibb,M.J., Buttner,M.J., Chater,K.F. and Hopwood,D.A. (2000) *Practical Streptomyces Genetics*. John Innes Foundation, Norwich, UK.
12. Bishop,A., Fielding,S., Dyson,P. and Herron,P. (2004) Systematic insertional mutagenesis of a streptomycete genome: a link between osmoadaptation and antibiotic production. *Genome Res.*, **14**, 893–900.
13. Kois,A., Swiatek,M., Jakimowicz,D. and Zakrzewska-Czerwinska,J. (2009) SMC protein-dependent chromosome condensation during aerial hyphal development in Streptomyces. *J. Bacteriol.*, **191**, 310–319.
14. Chakraburtty,R. and Bibb,M. (1997) The ppGpp synthetase gene (relA) of *Streptomyces coelicolor* A3(2) plays a conditional role in antibiotic production and morphological differentiation. *J. Bacteriol.*, **179**, 5854–5861.
15. Yanisch-Perron,C., Vieira,J. and Messing,J. (1985) Improved M13 phage cloning vectors and host strains: nucleotide sequences of the M13mp18 and pUC19 vectors. *Gene*, **33**, 103–119.
16. Flett,F., Mersinias,V. and Smith,C.P. (1997) High efficiency intergeneric conjugal transfer of plasmid DNA from *Escherichia coli* to methyl DNA-restricting streptomycetes. *FEMS Microbiol. Lett.*, **155**, 223–229.
17. Sun,J., Kelemen,G.H., Fernandez-Abalos,J.M. and Bibb,M.J. (1999) Green fluorescent protein as a reporter for spatial and temporal gene expression in *Streptomyces coelicolor* A3(2). *Microbiology*, **145(Pt 9)**, 2221–2227.
18. Fernandez Martinez,L., Bishop,A., Parkes,L., Del Sol,R., Salerno,P., Sevcikova,B., Mazurakova,V., Kormanec,J. and Dyson,P. (2009) Osmoregulation in *Streptomyces coelicolor*: modulation of SigB activity by OsaC. *Mol. Microbiol.*, **71**, 1250–1262.
19. Mistry,B.V., Del Sol,R., Wright,C., Findlay,K. and Dyson,P. (2008) FtsW is a dispensable cell division protein required for Z-ring stabilization during sporulation septation in *Streptomyces coelicolor*. *J. Bacteriol.*, **190**, 5555–5566.
20. Del Sol,R., Mullins,J.G., Grantcharova,N., Flardh,K. and Dyson,P. (2006) Influence of CrgA on assembly of the cell division protein FtsZ during development of *Streptomyces coelicolor*. *J. Bacteriol.*, **188**, 1540–1550.
21. Gust,B., Challis,G.L., Fowler,K., Kieser,T. and Chater,K.F. (2003) PCR-targeted Streptomyces gene replacement identifies a protein domain needed for biosynthesis of the sesquiterpene soil odor geosmin. *Proc. Natl Acad. Sci. USA*, **100**, 1541–1546.
22. Ausmees,N., Wahlstedt,H., Bagchi,S., Elliot,M.A., Buttner,M.J. and Flardh,K. (2007) SmeA, a small membrane protein with multiple functions in Streptomyces sporulation including targeting of a SpoIIIE/FtsK-like protein to cell division septa. *Mol. Microbiol.*, **65**, 1458–1473.
23. Ali,N., Herron,P.R., Evans,M.C. and Dyson,P.J. (2002) Osmotic regulation of the Streptomyces lividans thiostrepton-inducible promoter, ptipA. *Microbiology*, **148**, 381–390.
24. Werlang,I.C., Schneider,C.Z., Mendonca,J.D., Palma,M.S., Basso,L.A. and Santos,D.S. (2009) Identification of Rv3852 as a nucleoid-associated protein in Mycobacterium tuberculosis. *Microbiology*, **155**, 2652–2663.
25. Facey,P.D., Hitchings,M.D., Saavedra-Garcia,P., Fernandez-Martinez,L., Dyson,P.J. and Del Sol,R. (2009) *Streptomyces coelicolor* Dps-like proteins: differential dual roles in response to stress during vegetative growth and in nucleoid condensation during reproductive cell division. *Mol. Microbiol.*, **73**, 1186–1202.
26. Facey,P.D., Sevcikova,B., Novakova,R., Hitchings,M.D., Crack,J.C., Kormanec,J., Dyson,P.J. and Del Sol,R. The dpsA gene of *Streptomyces coelicolor*: induction of expression from a single promoter in response to environmental stress or during development. *PLoS One*, **6**, e25593.
27. Bharath,M.M., Ramesh,S., Chandra,N.R. and Rao,M.R. (2002) Identification of a 34 amino acid stretch within the C-terminus of histone H1 as the DNA-condensing domain by site-directed mutagenesis. *Biochemistry*, **41**, 7617–7627.
28. Christiansen,G., Pedersen,L.B., Koehler,J.E., Lundemose,A.G. and Birkelund,S. (1993) Interaction between the Chlamydia trachomatis histone H1-like protein (Hc1) and DNA. *J. Bacteriol.*, **175**, 1785–1795.
29. Paul,B.J., Berkmen,M.B. and Gourse,R.L. (2005) DksA potentiates direct activation of amino acid promoters by ppGpp. *Proc. Natl Acad. Sci. USA*, **102**, 7823–7828.
30. Chakraburtty,R., White,J., Takano,E. and Bibb,M. (1996) Cloning, characterization and disruption of a (p)ppGpp synthetase gene (relA) of *Streptomyces coelicolor* A3(2). *Mol. Microbiol.*, **19**, 357–368.
31. Jishage,M., Kvint,K., Shingler,V. and Nystrom,T. (2002) Regulation of sigma factor competition by the alarmone ppGpp. *Genes Dev.*, **16**, 1260–1270.
32. Kang,J.G., Paget,M.S., Seok,Y.J., Hahn,M.Y., Bae,J.B., Hahn,J.S., Kleanthous,C., Buttner,M.J. and Roe,J.H. (1999) RsrA, an anti-sigma factor regulated by redox change. *EMBO J.*, **18**, 4292–4298.
33. Paget,M.S., Molle,V., Cohen,G., Aharonowitz,Y. and Buttner,M.J. (2001) Defining the disulphide stress response in *Streptomyces coelicolor* A3(2): identification of the sigmaR regulon. *Mol. Microbiol.*, **42**, 1007–1020.
34. Perederina,A., Svetlov,V., Vassylyeva,M.N., Tahirov,T.H., Yokoyama,S., Artsimovitch,I. and Vassylyev,D.G. (2004) Regulation through the secondary channel—structural framework for ppGpp-DksA synergism during transcription. *Cell*, **118**, 297–309.
35. Balke,V.L. and Gralla,J.D. (1987) Changes in the linking number of supercoiled DNA accompany growth transitions in *Escherichia coli*. *J. Bacteriol.*, **169**, 4499–4506.
36. Blot,N., Mavathur,R., Geertz,M., Travers,A. and Muskhelishvili,G. (2006) Homeostatic regulation of supercoiling sensitivity coordinates transcription of the bacterial genome. *EMBO Rep.*, **7**, 710–715.
37. Brown,L., Gentry,D., Elliott,T. and Cashel,M. (2002) DksA affects ppGpp induction of RpoS at a translational level. *J. Bacteriol.*, **184**, 4455–4465.
38. Feng,W.H., Mao,X.M., Liu,Z.H. and Li,Y.Q. The ECF sigma factor SigT regulates actinorhodin production in response to nitrogen stress in *Streptomyces coelicolor*. *Appl. Microbiol. Biotechnol.*, **92**, 1009–1021.
39. Costanzo,A., Nicoloff,H., Barchinger,S.E., Banta,A.B., Gourse,R.L. and Ades,S.E. (2008) ppGpp and DksA likely regulate the activity of the extracytoplasmic stress factor sigmaE in *Escherichia coli* by both direct and indirect mechanisms. *Mol. Microbiol.*, **67**, 619–632.